



ELSEVIER

Thermochimica Acta 360 (2000) 17–27

thermochimica
acta

www.elsevier.com/locate/tca

Synthesis, identification and thermal decomposition of double sulfites like $\text{Cu}_2\text{SO}_3 \cdot \text{MSO}_3 \cdot 2\text{H}_2\text{O}$ (M=Cu, Fe, Mn or Cd)

L.A. Silva^a, J.R. Matos^b, J.B. de Andrade^{a,*}

^aInstituto de Química, Universidade Federal da Bahia, Campus Universitário de Ondina, 40.170-290 Salvador, Bahia, Brazil

^bInstituto de Química, Universidade de São Paulo, 05508-900 São Paulo, Brazil

Received 22 January 2000; accepted 17 April 2000

Abstract

Double sulfites with empirical formula $\text{Cu}_2\text{SO}_3 \cdot \text{MSO}_3 \cdot 2\text{H}_2\text{O}$ (where M is Cu, Fe, Mn, or Cd) were obtained by saturation with sulfur dioxide gas of an aqueous mixture of M^{II} sulfate and copper sulfate at room temperature. The salts obtained were identified by infrared spectra, X-ray powder diffraction and elemental analysis. The compounds studied are isostructural with the Cu^{II} replacement by Mn^{II} , Fe^{II} , and Cd^{II} in Chevrel's salt ($\text{Cu}_2\text{SO}_3 \cdot \text{CuSO}_3 \cdot 2\text{H}_2\text{O}$). The thermal behavior of the double sulfites was evaluated by thermogravimetry analysis (nitrogen and air atmospheres) and differential scanning calorimetry. These salts are thermally stable up to 200°C. The structures of sulfite ion coordination influence strongly the course of the thermal decomposition. The sulfite species coordinated to the metal through the oxygen are easier oxidized to sulfate than sulfur-coordinated species, leading to preferential formation of $\text{M}^{\text{II}}\text{SO}_4$ and Cu_2O in the first step. The weight gain relative to the second step can be due to oxidation of Cu_2O to CuO and/or oxidation of $\text{M}^{\text{II}}\text{SO}_3$ to $\text{M}^{\text{II}}\text{SO}_4$ probably by self-generated atmosphere formed by dense volatile products liberated in the latter step. © 2000 Elsevier Science B.V. All rights reserved.

Keywords: Double sulfites; Chevrel's salt; Thermal behavior; TGA; DSC

1. Introduction

The atmospheric corrosion and catalytic oxidation of SO_2 have been studied for more than a century and it was generally believed that the major S species in the atmospheric environment were H_2S , SO_2 , or particulate SO_4^{-2} . There is evidence, however, that a significant portion of the airborne S species emitted into the environment may be particulate SO_3^{-2} [1]. More recent studies indicated that solid metal sulfites and sulfite complexes in solution may play a role as intermediaries in these oxidation processes [2–4];

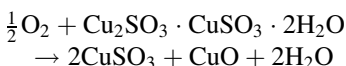
but there is no consensus about reaction rates, rate laws or mechanisms. Thus, metal sulfites may be used as model compounds to elucidate the reactions involving S^{IV} .

The mixed valence copper sulfite, $\text{Cu}_2\text{SO}_3 \cdot \text{CuSO}_3 \cdot 2\text{H}_2\text{O}$, Chevrel's salt, was used as a model compound for characterizing sulfite stability on particle surface exposed to air by monitoring the X-ray photoelectronic spectroscopy (XPS) for more than 600 days [5]. Several surface reactions of Chevrel's salt exposed to air with O_2 , including possible oxidation of S^{IV} to S^{VI} and Cu^{I} to Cu^{II} , were considered. Since no SO_4^{-2} was detected by XPS in the final products, the reaction below is most likely to occur. This is consistent with the conclusions of Eatough et al. [1] that atmospheric S^{IV} species,

* Corresponding author.

E-mail address: jailsong@ufba.br (J.B. de Andrade)

such as sulfites, may have long residence times in the environment.



Several experiments were carried out to evaluate the thermal behavior of the alkaline-earth sulfite and transition metal sulfite [6–10] using thermogravimetry analysis (TGA) and derivative thermal analysis (DTA). In most cases, hydrated sulfites decompose with loss of water and then, or simultaneously, SO_2 , followed by sulfation reaction. The final products are usually oxides of the respective metals. Thus far, the effect of atmosphere by their heating has not been studied.

The study of thermal behavior of mixed valence sulfite may help to understand the stability of the S^{IV} compounds in the environment. Nevertheless, there are no data about thermal analysis of this kind of sulfites in literature. Hence, the main objective of this investigation is to explore the thermal behavior of double sulfites of Cu^{I} with a transition divalent metal M^{II} (where $\text{M}=\text{Cu}^{\text{II}}, \text{Mn}^{\text{II}}, \text{Fe}^{\text{II}},$ and Cd^{II}), like $\text{Cu}_2\text{SO}_3 \cdot \text{MSO}_3 \cdot 2\text{H}_2\text{O}$, on heating up to 25–1100°C in nitrogen and air atmospheres, using TGA and differential scanning calorimetry (DSC). In this work, we will pay special attention to the M^{II} cation influence in the thermal decomposition of these compounds.

2. Experimental

2.1. Preparation of the compounds

Copper, copper and manganese, copper and iron or copper and cadmium sulfate solutions (see compositions in Table 1) were saturated with sulfur dioxide gas

at room temperature to give solutions with pH of approximately 1. These solutions, contained in a erlenmeyer, were heated to $78 \pm 2^\circ\text{C}$. Under fast mixing provided by a magnetic stirrer, the pH of the solutions were raised to 3.0–3.5 by dropwise addition of a 20% sodium carbonate solution. The precipitation of the complex sulfites starts at about pH 3.0. The crystalline materials were immediately filtered and washed with deionized water and rinsed with alcohol, followed by air drying [11,12].

2.2. Chemical analysis

Total copper, manganese, iron, and cadmium were determined using an ICP/AES ARL, model 3410. Sulfur analysis was performed by the Shöniger volumetric method.

2.3. Infrared absorption spectrum

Infrared spectra were recorded using an FTIR spectrometer (BOMEM), model MB-102.

2.4. X-ray diffraction

The X-ray powder diffraction patterns were obtained using a SIEMENS diffractometer, model D5000.

2.5. Thermal analysis

Thermogravimetric (TG) analyses were performed using a Shimadzu TGA-50H thermobalance, in nitrogen and air dynamic atmospheres with a flow rate of 50 ml min^{-1} at a heating rate of $10^\circ\text{C min}^{-1}$ over the range 25–1100°C and using 10 mg of sample in an alumina cell. The DSC was performed using a

Table 1
Composition of the starting solutions

Double sulfite	$\text{MSO}_4 \cdot x\text{H}_2\text{O}^{\text{a}}$ (g)				Vol. solution (ml)
	Cu	Mn	Fe	Cd	
$\text{Cu}_2\text{SO}_3 \cdot \text{CuSO}_3 \cdot 2\text{H}_2\text{O}$	2.0	–	–	–	50
$\text{Cu}_2\text{SO}_3 \cdot \text{MnSO}_3 \cdot 2\text{H}_2\text{O}$	1.0	6.2	–	–	50
$\text{Cu}_2\text{SO}_3 \cdot \text{FeSO}_3 \cdot 2\text{H}_2\text{O}$	1.0	–	12.2	–	50
$\text{Cu}_2\text{SO}_3 \cdot \text{CdSO}_3 \cdot 2\text{H}_2\text{O}$	1.0	–	–	10.2	50

^a Cu ($x=5$), Mn ($x=1$), Fe ($x=7$), Cd ($x=\frac{8}{3}$).

Shimadzu DSC-50 thermal analyzer. DSC curves were obtained in nitrogen dynamic atmosphere with flow rate of 50 ml min^{-1} with masses of 2 mg at a heating rate of $10^\circ\text{C min}^{-1}$ from ambient temperature to 550°C . The reference was a pure aluminum cell.

3. Results and discussion

3.1. Characterization of the compounds

According to elemental analysis results (Table 2) of the double sulfites of Cu^{I} with divalent cations, it could be confirmed that their general empirical formula is $\text{Cu}_2\text{SO}_3 \cdot \text{MSO}_3 \cdot 2\text{H}_2\text{O}$, where M is Cu^{II} , Mn^{II} , Fe^{II} , and Cd^{II} .

The crystalline structure of $\text{Cu}_2\text{SO}_3 \cdot \text{CuSO}_3 \cdot 2\text{H}_2\text{O}$ (Chevreul's salt) was determined by Kiergaard and Nyberg [13]. The structure was described in terms of coordination polyhedra: SO_3 trigonal pyramids, $\text{Cu}^{\text{I}}\text{O}_3\text{S}$ tetrahedra and $\text{Cu}^{\text{II}}\text{OH}(\text{H}_2\text{O})_2$ octahedra. The polyhedra are linked together giving a three-dimensional network (Fig. 1).

The X-ray diffraction data (Table 3) provided evidence for Cu^{II} replacement by Mn^{II} , Fe^{II} , and Cd^{II} in Chevreul's salt. It is seen that the patterns from the substituted sulfites resemble that of Chevreul's salt with minor changes in "d" spacings.

The free sulfite ion presents C_{3v} symmetry and gives rise to four infrared active fundamental modes: ν_1 (symmetric stretch), ν_2 (symmetric bend), ν_3 (asym-

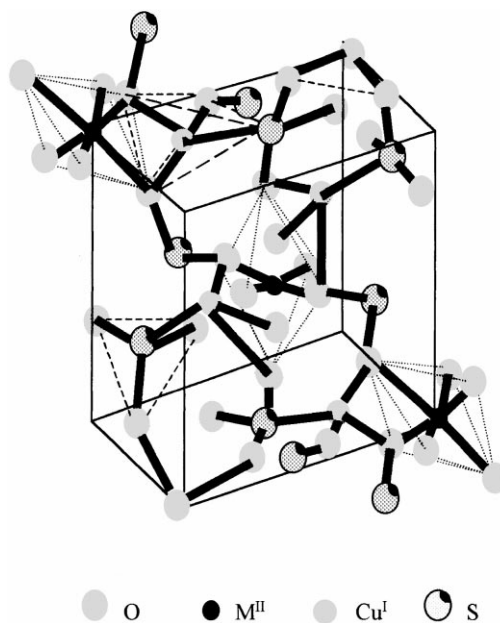
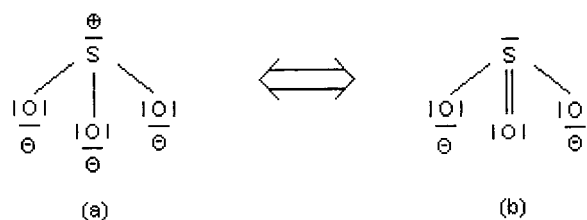


Fig. 1. Unit cell of the Chevreul's salt.

metric stretch), and ν_4 (asymmetric bend) [14]. The two asymmetric modes are doubly degenerated. Assuming that the 3d orbitals of sulfur participate in bonding, the S–O bond shows a partial double bond character and two of the resonance structures of the sulfite ion can be written:



Consequently a decrease in the stretching frequency following the decrease of the bond order would be expected in a compound with oxygen coordination (a); the symmetry of the group is changed to C_s and the number of infrared active fundamental modes is increased to six due to the removal of degeneracy from ν_3 and ν_4 . If the sulfite group is coordinated to the metal through sulfur (b) the C_{3v} symmetry is essentially preserved, but the stretching modes should shift to higher frequencies when compared with the free ion because of the higher bond order [14].

Table 2
Composition of the obtained compounds

Double sulfite	Element	Calculated (%)	Found (%)
$\text{Cu}_2\text{SO}_3 \cdot \text{CuSO}_3 \cdot 2\text{H}_2\text{O}$	Cu_{total}	49.3	48.8
	S	16.57	16.65
$\text{Cu}_2\text{SO}_3 \cdot \text{MnSO}_3 \cdot 2\text{H}_2\text{O}$	Cu	33.6	33.5
	Mn	14.5	14.7
	S	16.94	16.80
$\text{Cu}_2\text{SO}_3 \cdot \text{FeSO}_3 \cdot 2\text{H}_2\text{O}$	Cu	33.5	33.2
	Fe	14.7	14.2
	S	16.90	16.70
$\text{Cu}_2\text{SO}_3 \cdot \text{CdSO}_3 \cdot 2\text{H}_2\text{O}$	Cu	30.2	29.5
	Cd	25.9	24.9
	S	14.71	13.68

Table 3
X-ray powder diffraction data of d (Å)

$\text{Cu}_2\text{SO}_3 \cdot \text{CuSO}_3 \cdot 2\text{H}_2\text{O}$	$\text{Cu}_2\text{SO}_3 \cdot \text{MnSO}_3 \cdot 2\text{H}_2\text{O}$	$\text{Cu}_2\text{SO}_3 \cdot \text{FeSO}_3 \cdot 2\text{H}_2\text{O}$	$\text{Cu}_2\text{SO}_3 \cdot \text{CdSO}_3 \cdot 2\text{H}_2\text{O}$
5.6828	5.7046	5.6289	
4.9704	4.7791	4.7638	4.7862
4.6596	4.6235	4.6021	
4.1834	4.0752	4.0477	4.0959
3.9832	3.9569	3.9258	
3.5337	3.5504	3.5337	3.6192
	3.4687	3.4607	
3.0681	3.2488	3.1973	3.0222
2.9780	2.9926	2.9780	
2.7928	2.8474	2.8368	2.8742
			2.5956
2.5390	2.5815	2.5750	2.5513
2.5101	2.5122	2.4960	2.5153
2.4780			
	2.0850	2.0714	
2.2618			2.2480

According to Nyberg and Larson [14] the structure of the sulfite compounds can be divided into three groups after the sulfite ion coordination: (I) compounds without sulfur coordination (below 975 cm^{-1}); (II) compounds with both sulfur and oxygen coordination (above and below 975 cm^{-1}); (III) compounds with dominant sulfur coordination (above 975 cm^{-1}). The $\text{Cu}_2\text{SO}_3 \cdot \text{CuSO}_3 \cdot 2\text{H}_2\text{O}$ (Chevreul's salt) belongs to the second group with both metal–sulfur bonds and metal–oxygen bonds [12–14]. The spectrum of this compound shows stretching frequencies of high intensity above and below 975 cm^{-1} (Fig. 2).

The infrared spectra of $\text{Cu}_2\text{SO}_3 \cdot \text{MnSO}_3 \cdot 2\text{H}_2\text{O}$, $\text{Cu}_2\text{SO}_3 \cdot \text{FeSO}_3 \cdot 2\text{H}_2\text{O}$, and $\text{Cu}_2\text{SO}_3 \cdot \text{CdSO}_3 \cdot 2\text{H}_2\text{O}$ (Fig. 2) are similar to that of Chevreul's salt and may be assigned in a similar way. The vibrational bands of the sulfite group were assigned by comparison with literature data. All four fundamental modes of vibration of the sulfite ion were identified (Table 4) [12–14].

3.2. Thermal behavior

3.2.1. $\text{Cu}_2\text{SO}_3 \cdot \text{CuSO}_3 \cdot 2\text{H}_2\text{O}$

According to the TG and DSC curves (Figs. 3a and 4) the thermal decomposition of the Chevreul's salt in nitrogen atmosphere takes place in four stages. In the first one the dehydration of the compound occurs in a

single step ($200\text{--}290^\circ\text{C}$) with one endothermic peak followed by one exothermic peak (Fig. 4), which means that in this step the compound loses the two water molecules and SO_2 with redox reactions occurring simultaneously to form $\text{CuSO}_4 \cdot \text{Cu}_2\text{O}$. The second

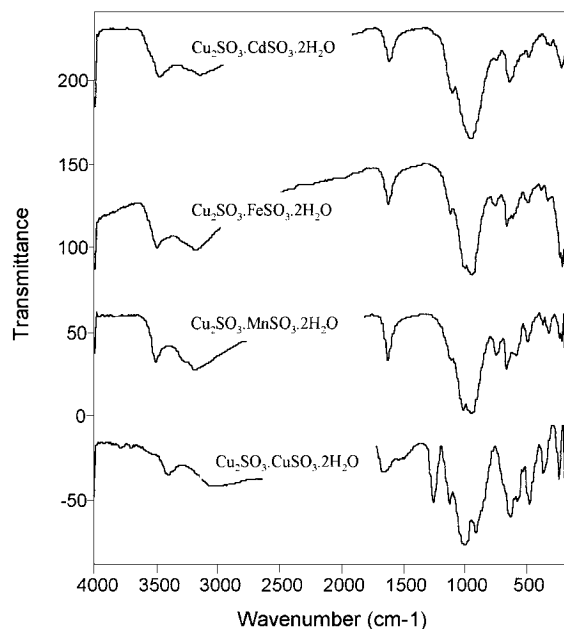
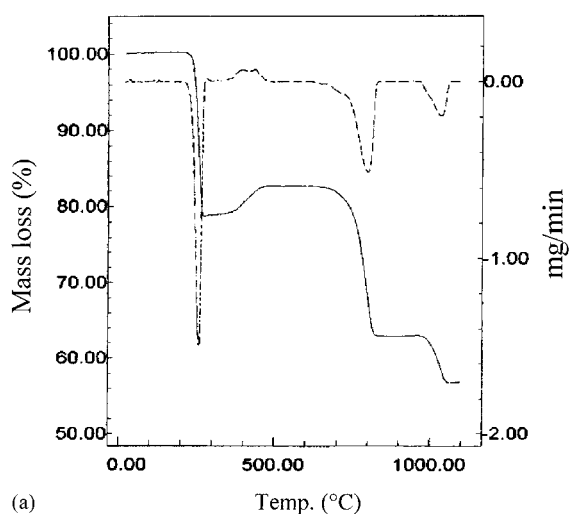


Fig. 2. Infrared spectra of the double sulfites, $\text{Cu}_2\text{SO}_3 \cdot \text{MSO}_3 \cdot 2\text{H}_2\text{O}$.

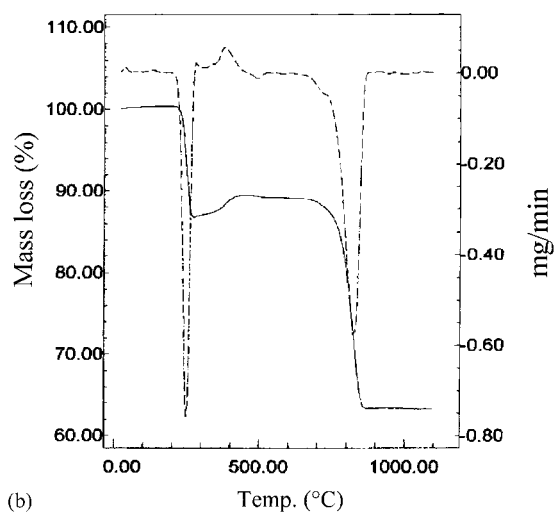
Table 4
Observed infrared frequencies (cm^{-1})

Compound	Assignment of SO_3^{a}		
	ν_1 and ν_3	ν_2	ν_4
$\text{Cu}_2\text{SO}_3 \cdot \text{CuSO}_3 \cdot 2\text{H}_2\text{O}$	1119m, 1024m, 993s, 974s	620m	475m
$\text{Cu}_2\text{SO}_3 \cdot \text{MnSO}_3 \cdot 2\text{H}_2\text{O}$	1120m, 1012s, 938s	667m, 619m	495m
$\text{Cu}_2\text{SO}_3 \cdot \text{FeSO}_3 \cdot 2\text{H}_2\text{O}$	1118m, 1012s, 931s	662m, 620m	497m
$\text{Cu}_2\text{SO}_3 \cdot \text{CdSO}_3 \cdot 2\text{H}_2\text{O}$	1114m, 993s, 965s	653s, 618m	479m

^a s=strong; m=medium.



(a)



(b)

Fig. 3. TG curves for the thermal decomposition of $\text{Cu}_2\text{SO}_3 \cdot \text{CuSO}_3 \cdot 2\text{H}_2\text{O}$ in (a) nitrogen and (b) air atmospheres.

stage shows a weight gain; the exothermic peak in DSC curve indicates that a oxidation reaction takes place in this step, even in nitrogen atmosphere, to form CuO . According to Duval [15] the oxidation of Cu_2O begins at about 285°C and near 350°C the conversion is practically complete. Oxygen comes from decomposition gases of the latter step. The compound formed ($\text{CuSO}_4 \cdot 2\text{CuO}$) does not show weight change until 600°C . However, the DSC curve shows one exothermic peak at about 515°C , which is characteristic of a crystal transition. In the third stage, thermal decomposition of copper sulfate to form CuO takes place. The copper(II) oxide begins to be reduced to copper(I) oxide at about 900°C .

The thermal behavior of $\text{Cu}_2\text{SO}_3 \cdot \text{CuSO}_3 \cdot 2\text{H}_2\text{O}$ in air atmosphere was also evaluated (Fig. 3b). In the first stage, the weight loss is smaller than the other one in nitrogen atmosphere. The infrared spectra show that

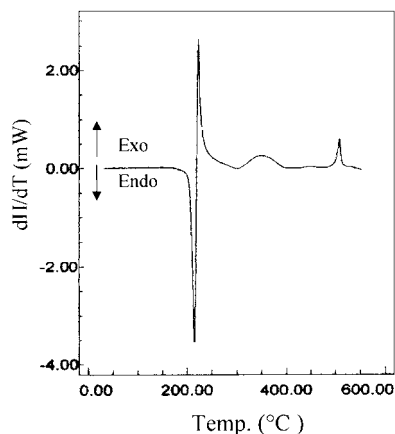


Fig. 4. DSC curve of $\text{Cu}_2\text{SO}_3 \cdot \text{CuSO}_3 \cdot 2\text{H}_2\text{O}$.

part of sulfite (Cu_2SO_3) is not converted to Cu_2O in this step, as it was observed in nitrogen atmosphere. The Cu_2O formation may be inhibited by air atmosphere. The remaining CuSO_3 is not oxidized to sulfate (see IR spectra, Fig. 5); this fact may be explained by sulfite coordination. The SO_3^{2-} coordinated through the oxygen is usually oxidized easier than that coordinated through the sulfur [10]. The

product obtained up to 270°C shows a sulfite band above 975 cm^{-1} in the infrared spectrum, characteristic of sulfur-coordinated species [14]. In the next stage, a weight gain takes place as a result of the oxidation of Cu_2O to CuO . Thus, the remaining copper sulfite has SO_3^{2-} coordinated through sulfur to the metal at temperature up to 600°C , this bonding is kept at about 680°C . The final product is CuO .

3.2.2. $\text{Cu}_2\text{SO}_3 \cdot \text{MnSO}_3 \cdot 2\text{H}_2\text{O}$

TG and DSC curves of $\text{Cu}_2\text{SO}_3 \cdot \text{MnSO}_3 \cdot 2\text{H}_2\text{O}$ are shown in Figs. 6 and 7, respectively. The TG curve profile of $\text{Cu}_2\text{SO}_3 \cdot \text{MnSO}_3 \cdot 2\text{H}_2\text{O}$ is similar to

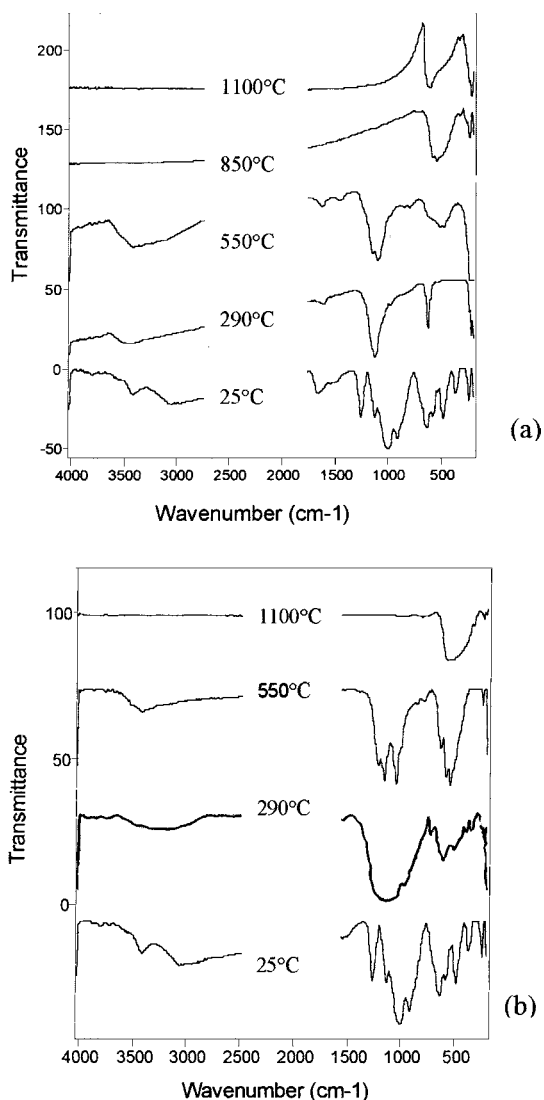


Fig. 5. IR spectra of $\text{Cu}_2\text{SO}_3 \cdot \text{CuSO}_3 \cdot 2\text{H}_2\text{O}$ and their intermediate compounds obtained from their thermal decomposition in (a) nitrogen and (b) air atmospheres.

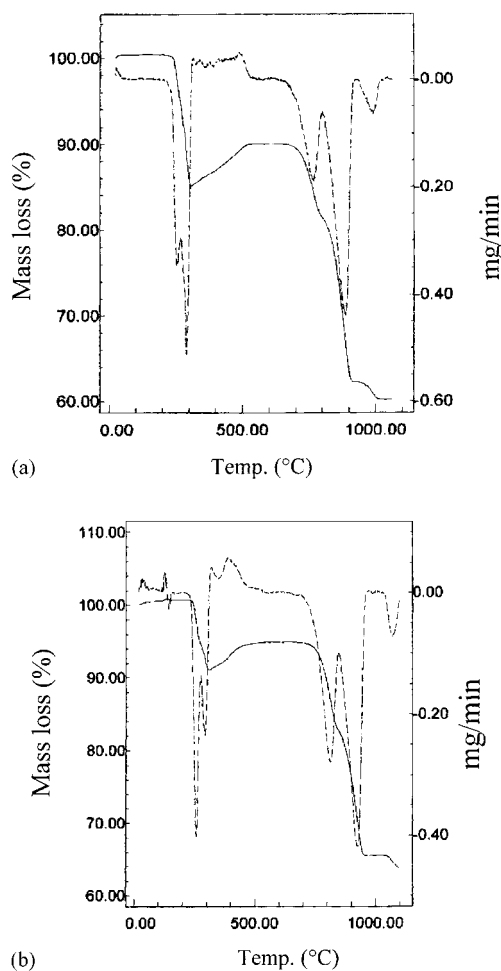
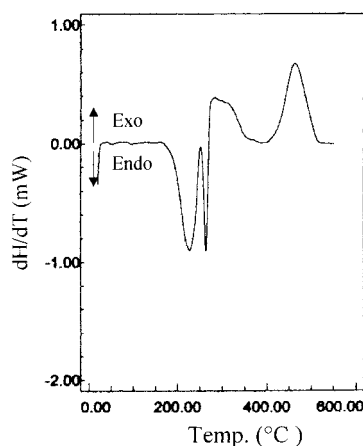
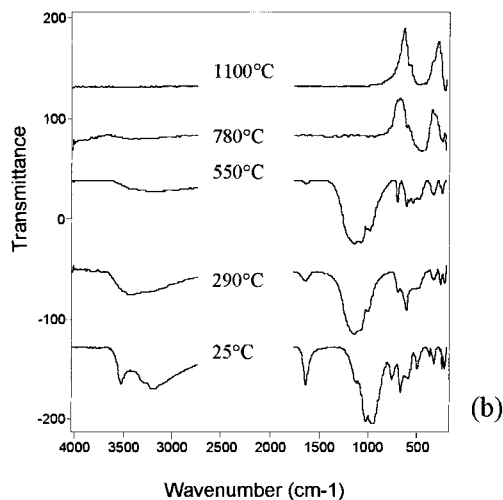
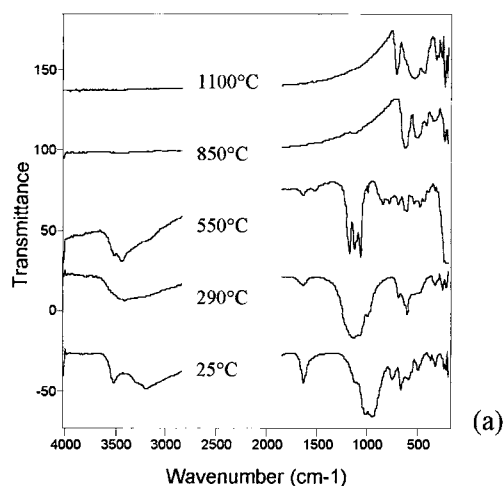


Fig. 6. TG curves for the thermal decomposition of $\text{Cu}_2\text{SO}_3 \cdot \text{MnSO}_3 \cdot 2\text{H}_2\text{O}$ in (a) nitrogen and (b) air atmospheres.

Fig. 7. DSC curve of $\text{Cu}_2\text{SO}_3 \cdot \text{MnSO}_3 \cdot 2\text{H}_2\text{O}$.Fig. 8. IR spectra of $\text{Cu}_2\text{SO}_3 \cdot \text{MnSO}_3 \cdot 2\text{H}_2\text{O}$ and their intermediate compounds obtained from their thermal decomposition in (a) nitrogen and (b) air atmospheres.

Chevreur's salt decomposition (Fig. 6). However, the dehydration of this compound takes place in two steps to form the anhydrous salt ($\text{Cu}_2\text{SO}_3 \cdot \text{MnSO}_3$) at about 270°C, but it was impossible to isolate it. Above 270°C the TG curve in nitrogen atmosphere (Fig. 6a) shows another weight loss corresponding to the SO_2 evolution, and disproportionation reaction must occur to form MnSO_4 , $\text{CuSO}_3 \cdot \text{MnSO}_3$, and Cu_2O (see IR spectra, Fig. 8). In the next step, Cu_2O is oxidized to CuO , and the remaining MnSO_3 is oxidized too; however, CuSO_3 is sulfur-coordinated, so it is not oxidized to sulfate. At about 850°C, CuO and CuMnO_2 are formed; above this temperature CuO is reduced to Cu_2O .

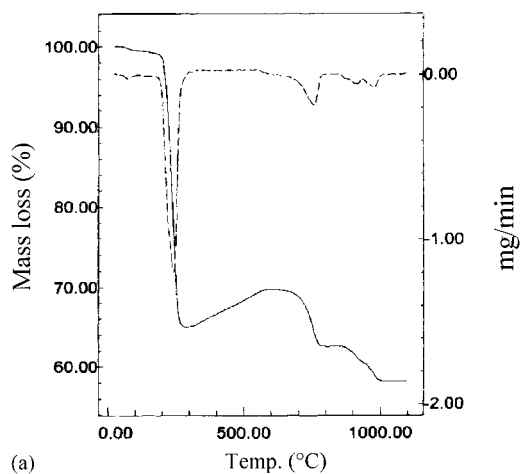
In air atmosphere (Fig. 6b), the anhydrous salt ($\text{Cu}_2\text{SO}_3 \cdot \text{MnSO}_3$) is oxidized to form $\text{Cu}_2\text{SO}_3 \cdot \text{MnSO}_4$; but these two compounds were not isolated, at least in the present study, because they are not stable in contact with humid air. At about 850°C, CuO and MnO_2 are formed. The final products are CuO and $\text{Cu}_{1.4}\text{Mn}_{1.6}\text{O}_4$.

3.2.3. $\text{Cu}_2\text{SO}_3 \cdot \text{FeSO}_3 \cdot 2\text{H}_2\text{O}$

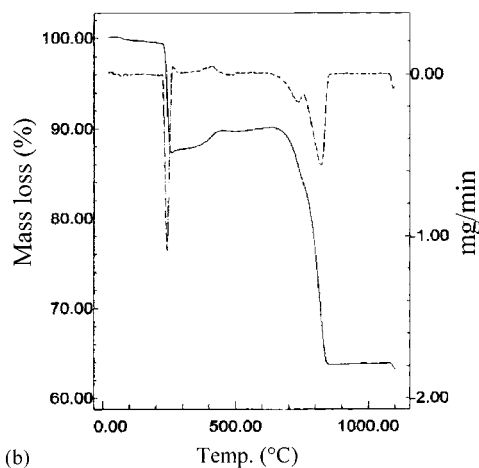
TG and DSC curves of $\text{Cu}_2\text{SO}_3 \cdot \text{FeSO}_3 \cdot 2\text{H}_2\text{O}$ are shown in Figs. 9 and 10, respectively. TG curves in nitrogen and air atmosphere show the same behavior of the Chevreur's salt decomposition (Fig. 9). In nitrogen atmosphere (Fig. 9a), the first weight loss is matched to the loss of two water molecules and a disproportionation reaction to form FeSO_4 , FeO , and Cu_2O (Fig. 11). In the next stage, the Cu_2O is oxidized

to CuO , even in nitrogen atmosphere like Chevreur's salt. The compounds formed are stable at about 700°C whereas they are decomposed to CuO and CuFe_2O_4 . Above 780°C, these compounds are reduced to Cu_2O and CuFeO_2 .

The thermal behavior in air atmosphere (Fig. 9b) is similar to that in nitrogen atmosphere; nevertheless, no FeO is formed in the first stage and there is CuSO_3 remaining like Chevreur's salt decomposition (Fig. 11). The second step shows a weight gain resulting in the oxidation of Cu_2O . The compounds



(a)



(b)

Fig. 9. TG curves for the thermal decomposition of $\text{Cu}_2\text{SO}_3 \cdot \text{FeSO}_3 \cdot 2\text{H}_2\text{O}$ in (a) nitrogen and (b) air atmospheres.

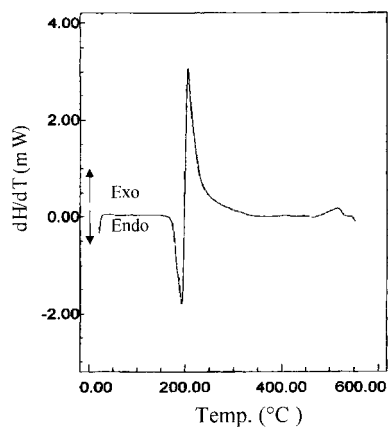
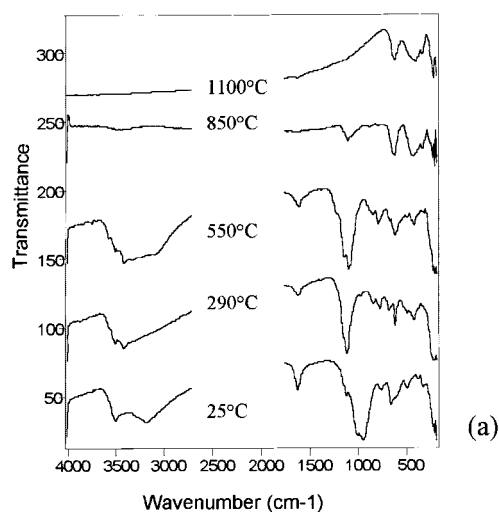
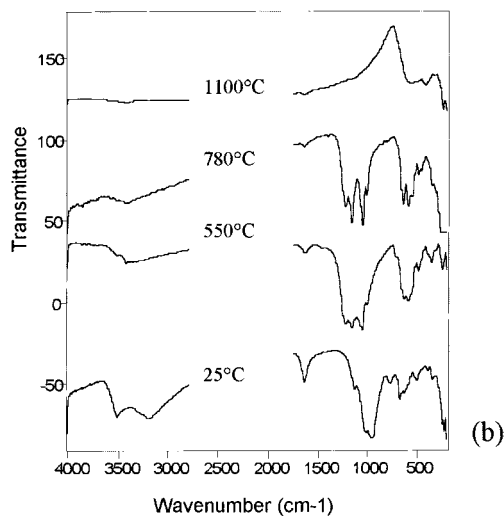


Fig. 10. DSC curve of $\text{Cu}_2\text{SO}_3 \cdot \text{FeSO}_3 \cdot 2\text{H}_2\text{O}$.



(a)



(b)

Fig. 11. IR spectra of $\text{Cu}_2\text{SO}_3 \cdot \text{FeSO}_3 \cdot 2\text{H}_2\text{O}$ and their intermediate compounds obtained from their thermal decomposition in (a) nitrogen and (b) air atmospheres.

formed are stable at about 650°C , whereas they are decomposed to form CuO and CuFe_2O_4 .

3.2.4. $\text{Cu}_2\text{SO}_3 \cdot \text{CdSO}_3 \cdot 2\text{H}_2\text{O}$

As observed in TG and DSC curves (Figs. 12 and 13), this compound begins to lose the water molecules at about 190°C . The dehydration occurs in one step in air and two steps in nitrogen atmosphere. The first exothermic peak in DSC curve (Fig. 13) suggests a disproportionation reaction of anhydrous salt to form

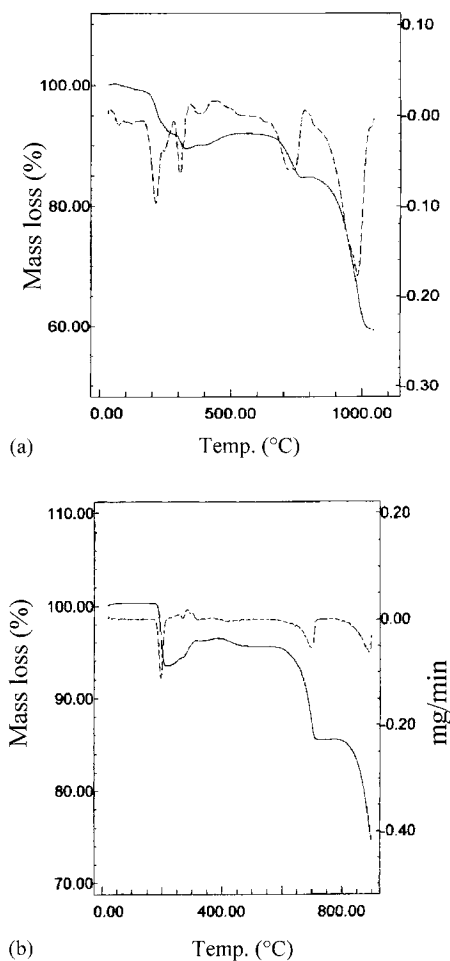


Fig. 12. TG curves for the thermal decomposition of $\text{Cu}_2\text{SO}_3 \cdot \text{CdSO}_3 \cdot 2\text{H}_2\text{O}$ in (a) nitrogen and (b) air atmospheres.

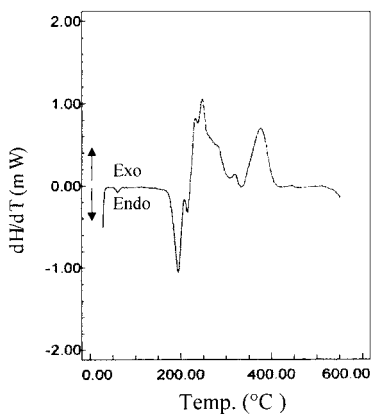


Fig. 13. DSC curve of $\text{Cu}_2\text{SO}_3 \cdot \text{CdSO}_3 \cdot 2\text{H}_2\text{O}$.

Cu_2O and $\text{CuSO}_3 \cdot \text{CdSO}_3$. The TG curve in nitrogen atmosphere (Fig. 12a) shows another weight loss up to 270°C that can be matched to SO_2 evolution, and the second exothermic peak in DSC curve indicates CdSO_4 formation (Fig. 13). At about 300°C , the sample begins to gain weight like the other double sulfites. The third exothermic peak indicates that oxidation takes place also in an inert atmosphere to

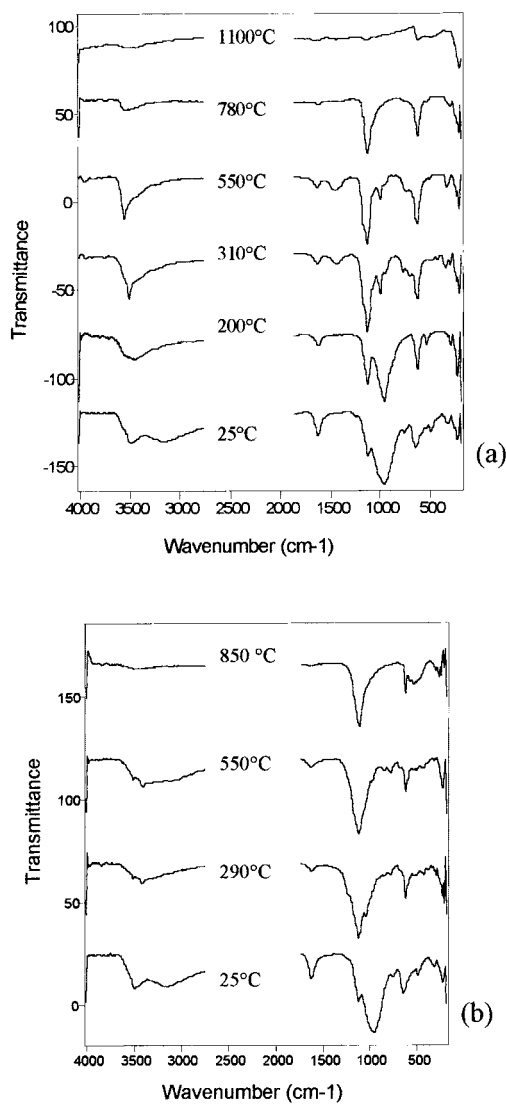
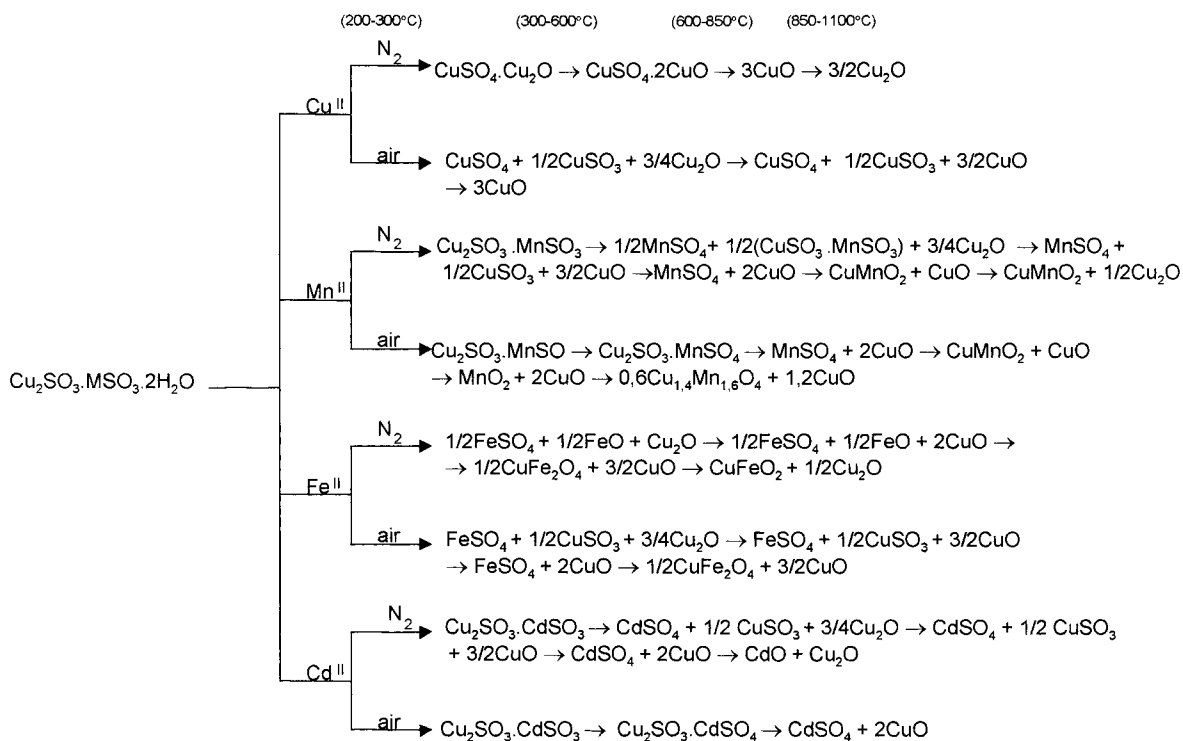


Fig. 14. IR spectra of $\text{Cu}_2\text{SO}_3 \cdot \text{CdSO}_3 \cdot 2\text{H}_2\text{O}$ and their intermediate compounds obtained from their thermal decomposition in (a) nitrogen and (b) air atmospheres.



Scheme 1.

form CuO. The product after this step at 500°C corresponds to CuO and CdSO₄. The final products of the thermal decomposition of this compound are Cu₂O and CdO.

In air atmosphere (Fig. 12b), the weight gain takes place immediately after dehydration and disproportionation reaction must occur (Fig. 14). The products formed are stable until 600°C, whereas they are decomposed to form CuO and CdSO₄. The latter is stable up to 906°C.

The thermal decomposition of the double sulfites are presented in Scheme 1.

The agreement between calculation and experimental mass change values suggested in the above scheme, was very good; the largest difference was only 1.76%. The formation of the oxides by thermal decomposition of the double sulfites are also in agreement with the X-ray powder diffraction patterns. On the other hand, the X-ray diffraction data obtained from the first and second stages did not allow to identify the intermediary compounds due to their high complexity. In the present work, it was difficult to distinguish sulfite,

sulfate, and sulfite sulfate phases on the basis of the chemical analysis or by thermoanalytical methods alone. IR spectroscopy is probably the most sensitive method to detect the sulfate ion in a sulfite matrix.

4. Conclusion

The double sulfites studied in this work are thermally stable up to 200°C in both atmospheres, nitrogen and air. The structures of sulfite ion coordination influence strongly the course of the thermal decomposition of these salts. According to the results the sulfite species coordinated to the metal through the oxygen atom are easier oxidized to sulfate than sulfur-coordinated species, leading to preferential formation of M^{II}SO₄ and Cu₂O in the first step of the thermal decomposition. The presence of Cu₂O in the solid residue indicates that SO₂ evolution, in the first step, takes place through the break of Cu^I-S and Cu^IO-S bonding. The weight gain relative to the second step is similar for all mixed valence sulfites studied, even in

inert atmosphere. This fact can be explained due to oxidation of Cu_2O to CuO and/or oxidation of $\text{M}^{\text{II}}\text{SO}_3$ to $\text{M}^{\text{II}}\text{SO}_4$ probably by self-generated atmosphere formed by dense volatile products liberated in the latter step.

Acknowledgements

The authors are indebted to CNPq, CAPES and FINEP for financial support, to Prof. Dr. Heloisa Andrade for analytical assistance, and Prof. Dr. Pedro Afonso de Paula Pereira and Prof. Dr. José Oscar Nogueira Reis for helpful discussions. LAS is supported by a CAPES fellowship.

References

- [1] D.J. Eatough, J.J. Christensen, N.L. Eatough, M.W. Hill, T.D. Major, N.F. Mangelson, M.E. Post, J.F. Ryder, L.D. Hansen, *Atmos. Environ.* 16 (1982) 1001.
- [2] M.H. Conklin, M.R. Hoffmann, *Environ. Sci. Technol.* 22 (1) (1988) 883.
- [3] M.H. Conklin, M.R. Hoffmann, *Environ. Sci. Technol.* 22 (2) (1988) 891.
- [4] M.H. Conklin, M.R. Hoffmann, *Environ. Sci. Technol.* 22 (3) (1988) 899.
- [5] X.B. Cox, R.W. Linton, A.H. Miguel, J.B. de Andrade, *Atmos. Environ.* 20 (1988) 1139.
- [6] H.A. Papazian, P.J. Pizzolato, J. Peng, *Thermochim. Acta* 5 (1972) 147.
- [7] Von H.D. Lutz, E. El Suradi, *Z. Anorg. Allg. Chem.* 425 (1976) 134.
- [8] W.D. Herrison, J.B. Gill, D.C. Goodall, *Polyhedron* 2 (1983) 153.
- [9] V.P. Verma, *Thermochim. Acta* 89 (1985) 363.
- [10] M. Ishihara, H. Matsui, G. Hashizume, *J. Therm. Anal.* 38 (1992) 1801.
- [11] R.R. Skarbo, M.J. Redman, Technical Report No. 16, Kennecott Copper Corporation, Ledgemont Laboratory, Lexington, MA, 1967.
- [12] L.A. Silva, S.J. Correia, C.R. Martins, J.B. de Andrade, *Química Nova* 21 (2) (1998) 151.
- [13] P. Kierkgaard, B. Nyberg, *Acta Chem. Scand.* 19 (1965) 2189.
- [14] B. Nyberg, P.L.O. Larson, *Acta Chem. Scand.* 27 (1973) 63.
- [15] C. Duval, *Inorganic Thermogravimetric Analysis*, 2nd Edition, Elsevier, Amsterdam, 1963.